Title: Additive Manufacturing via Tube Extrusion (AMTEx)

Authors: Nicholas Hopkins[a], Ruben Janse van Vuuren[a], Hadley Brooks[a]

[a] School of Engineering, Faculty of Science and Technology, University of Central Lancashire

Corresponding author: Hadley Brooks, hlbrooks1@uclan.ac.uk

Abstract:

Large scale Fused Filament Fabrication (FFF) is a growing area of interest within AM, with several unresolved problems: the volumetric cost of materials is high, the printing process is slow and low cooling rates result in unstable or sagging structures. This paper presents the concept of additive manufacturing via tube extrusion (AMTEx) as a means of overcoming these issues.

Using hollow tubes in place of solid extrusions means material use is reduced and cooling properties are vastly improved, allowing spans in excess of 400mm without sag. Conventional freeform extrusion relies on the use of six-axis robots to orientate the extruder nozzle tangentially to the toolpath. It was found that slight pressurisation of the inside of printed tubes allowed extrusion at more than 90° from the nozzle axis without tube collapse. Aside from reducing the possibility of robot-print collisions, this also allows the use of traditional 3D printing slicing software to generate printer toolpaths. It also opens the potential to use conventional three-axis machines, greatly increasing the applicability of printing with tubes. AMTEx tubes were found to be stronger under tension and bending compared to equivalent FFF parts and had significantly improved ductility.

Keywords: Additive Manufacturing; Tubes; Robot; Large; Self-supporting; 3D printing.

Abbreviations:

FFF – Fused Filament Fabrication

AMTEx – Additive Manufacturing via Tube Extrusion

1 Introduction:

The build volumes for additive manufacturing (AM) technologies are increasing in size, enabling new applications such as large moulds, boat hulls, automobile chassis and buildings [1-6]. Use of the search term ‘large 3D printer’ has increased 900% from 2012 to 2020 [7]. Fused Filament Fabrication (FFF) printers, which use thermoplastic feedstocks, are increasingly used for large parts, due to their relative simplicity and low costs. A downside to printing large thermoplastic parts is the high material costs and long print times [3, 8, 9].

Large nozzles and high extrusion rates are used to help reduce print times. However, volumetric extrusion rates are often restricted by how quickly the polymers can be melted, and how long they take to cool once deposited [10]. Extrusion tracks with large cross-sectional areas remain soft for a long time, inhibiting their ability to resist gravity and to rapidly support subsequent layers [8]. Active

air cooling is a common method to increase cooling rates; but can result in asymmetrical cooling, excessive part warping, and is not very effective for large (>1 cm²) cross-sections due to the poor thermal conductivity of polymers [5, 8].

This paper will demonstrate a method of extruding hollow tubes as a method of printing large parts with minimal material use. Tubes are naturally strong structures and offer superior self-supporting characteristics over rods with the same cross-sectional area. Tubes also have favourable cooling characteristics, benefitting freeform printing and bridging.

3D printing tubes and other coaxial structures, is an underdeveloped area of research, with prior focus on small scale applications such as tissue scaffolds and optical fibres [11, 12]. Robotic freeform printing is also underdeveloped with few commercial examples [6, 13-15]. To the author's knowledge this is the first paper to demonstrate freeform Additive Manufacturing via Tube Extrusion (AMTEx).

1.2 AMTEx Concepts

1.2.1 Mechanical properties of tubes

Tubes often occur in nature where high strength to weight ratios and efficient material use are required [16]. The favourable mechanical properties come from increased bending and torsional strength, as described by Eq. (1) and (2).

$$\sigma = \text{My/I, where } I_{Tube} = M(R_2^4 - R_1^4) \text{ or } I_{Rod} = MR^4 \quad (1)$$

$$\tau = \text{Tr/J, where } J_{Tube} = (\pi/2)(R_2^4 - R_1^4) \text{ or } J_{Rod} = (\pi/2)R^4 \quad (2)$$

A consequence of Eq. (1) and (2) is that a tube with double the radius of a rod, but with the same cross-sectional area (Figure 1), will be 16 times stronger in bending and torsion. Additionally, parts built with such tubes will require a quarter of the material compared to a part printed with solid rods.

1.2.2 Cooling properties of tubes

Extruding thermoplastics requires the polymer to be in a molten state as it exits the nozzle. This can be an issue when printing into air as the extrudate will sag under gravity. Additionally, when printing tall thin features, the accumulation of heat can be such that the whole structure becomes unstable, with lower layers unable to support higher layers. Printing with tubes can help reduce material use and/or increase surface area, which increases cooling rates over solid rods.

Figure 1 shows a 2D thermal simulation, performed using Solidworks Simulation, of a tube cooling compared to a rod of equal cross-sectional area. With a small amount of convective heat transfer on the surface, the PLA tube cools much faster than the rod. After 60 seconds the rod remains soft as it is still far above the glass transition temperature of PLA (60℃).

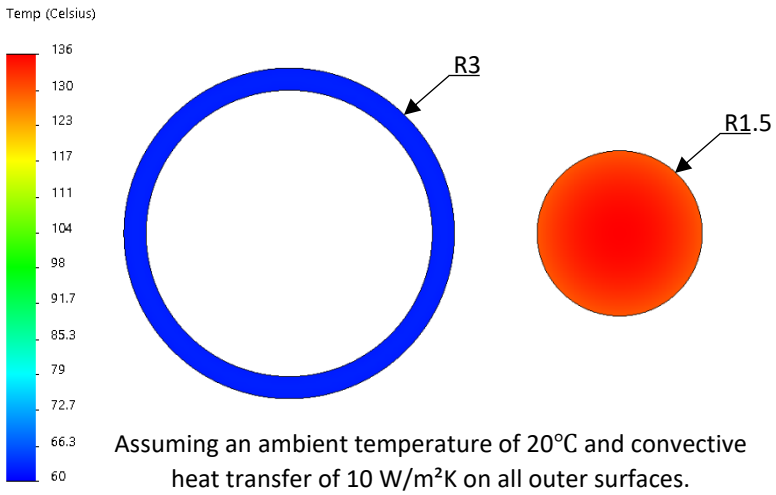

Figure 1. 2D thermal simulation showing the temperature of PLA tube and rod profiles with equal cross-sectional area (70.7mm²) after cooling from 240°C for 60 seconds.

1.2.3 3D printing strategies for tubes

The superior bending and torsional stiffness of tubes make them more amenable to freeform (non-layer based) printing strategies (Figure 2 left). These print strategies are often used in conjunction with robot arms, due to the extra rotational degrees of freedom (DOF) required to manipulate the extruder [6, 13-15, 17]. Despite the extra DOF, path planning is often complicated due to the increased risk of collisions between the robot and deposited material.

Tubes can also be printed using conventional layer-based printing strategies by pressurising the inside of the molten tube and allowing it to bend 90° as it comes out of the extruder nozzle (Figure 2 right). This is highly beneficial as it means conventional build preparation software, or slicers, can be used for toolpath planning.

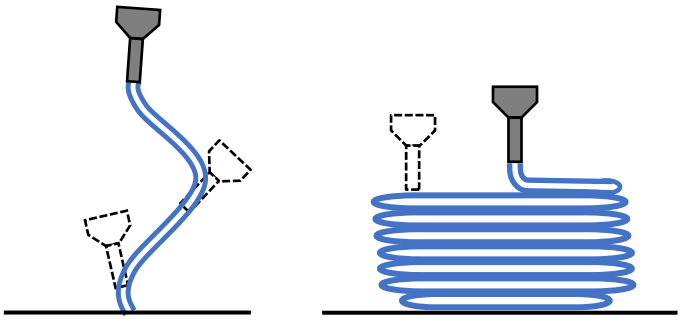

Figure 2. AMTEx print strategies: Freeform printing (left) and layer-based printing (right).

2 Robotic tube printing apparatus

To test the tube printing concept, a custom extruder was attached to a Universal Robots UR5 (Figure 3). The filament rolls and extruder motors were positioned on the second linkage and Bowden tubes were used to help reduce the load on the end of the arm.

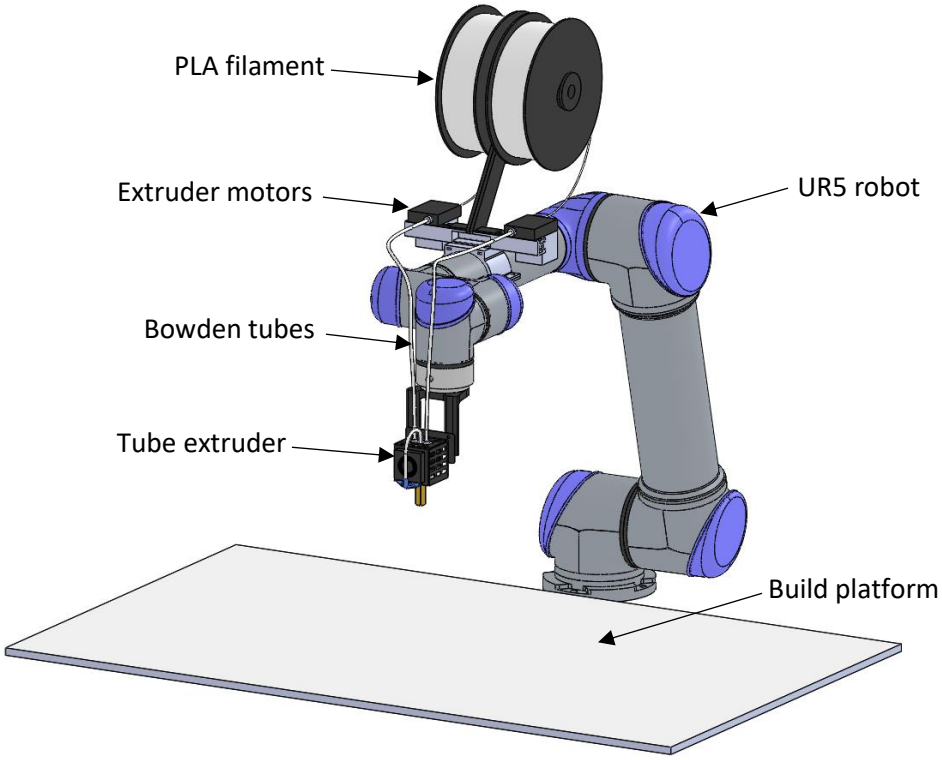

Figure 3. AMTEx apparatus.

2.1 End effector design

Two extruder stepper motors were used to allow higher extrusion rates and to provide mirror symmetry to the polymer flow. The filaments enter the cold end of the extruder via the Bowden tubes. Figure 4 shows the design of the tube extruder. The two polymer streams merge in the heater block and flow around a mandrel to form the molten tube. The channel inside the mandrel reduces thermal mass and provides a way to pressurise the inside of the tube.

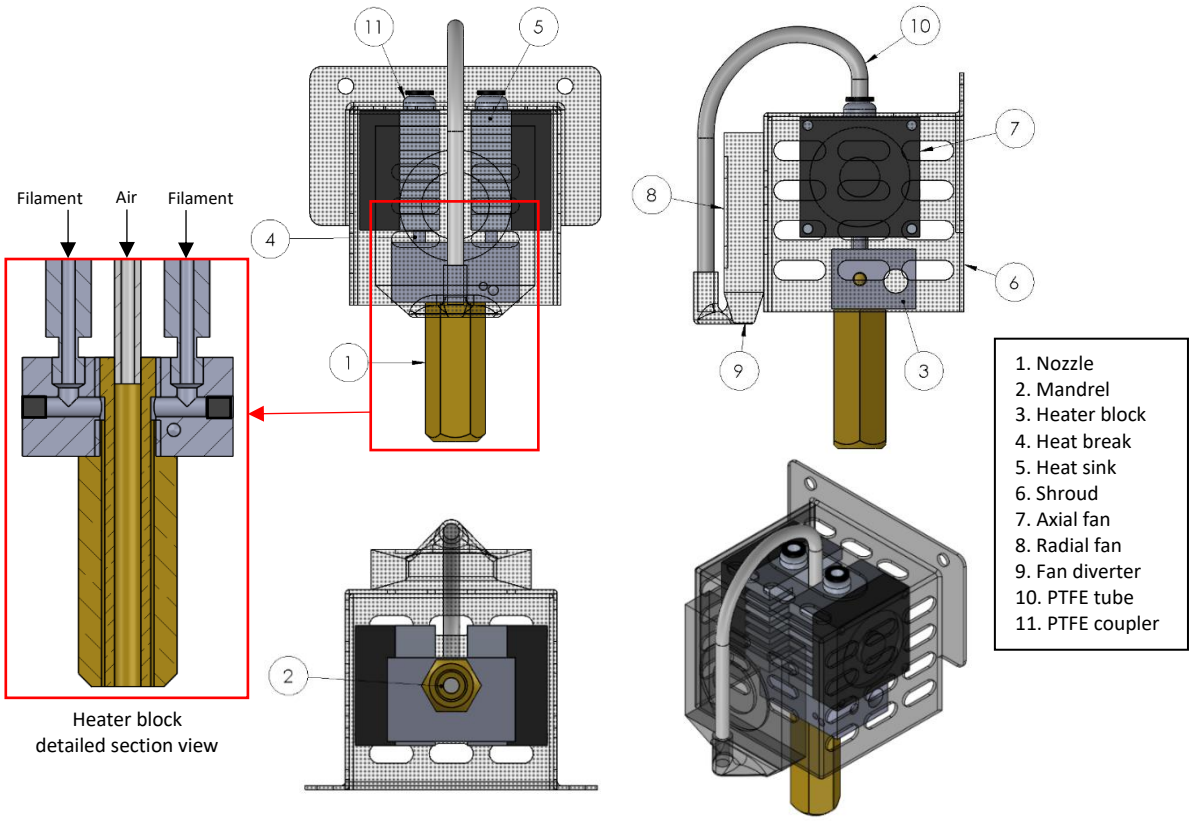

Figure 4. Design of the tube extruder (not to scale).

The outer diameter of the nozzle is 8mm with an inner diameter of 7mm. The extended nozzle is 50mm long and serves three functions; it improves reachability of the tool, gives time for the flow to homogenise, and allows the polymer to cool down slightly before exiting the nozzle orifice. The main restriction to flow occurs in the heater block, where the polymer needs to rapidly melt before flowing through a right-angle turn. Increasing the height of the heater block would likely aid in melting the polymer and increasing the extrusion rate.

Figure 5 shows how the temperature decreases from the heated block to the solidified tube.

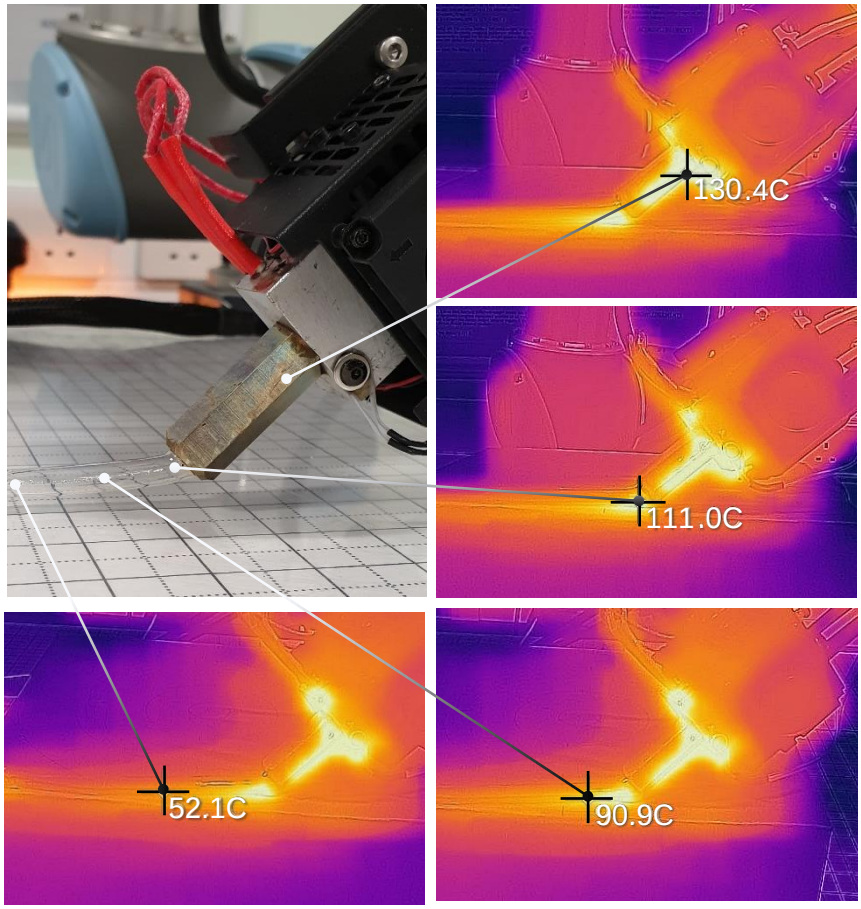

Figure 5. Thermal camera images of the extruder depositing a horizontal tube.

3. Print parameter study

Parameter tests were carried out by printing vertical PLA tubes. Extrusion rate (E), feed rate (F) and temperature (T) were varied to find acceptable parameter ranges (Figure 6).

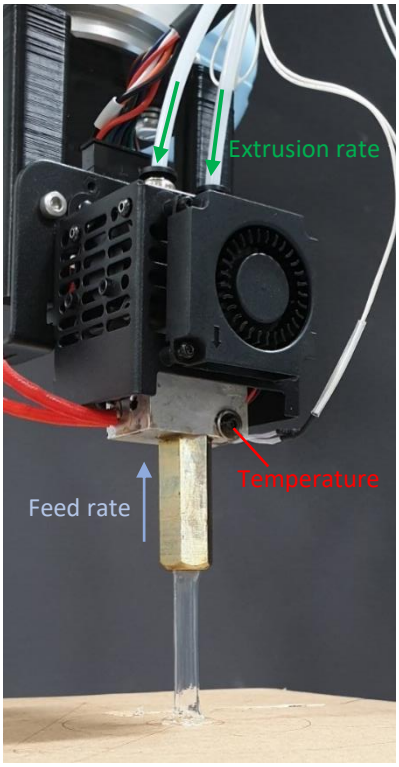

Figure 6. Experimental setup of the preliminary print tests.

In order to achieve stable freeform printing a balance between feed-rate and extrusion speed is required. The tubes were found to be elliptical with slightly inconsistent wall thicknesses (Figure 7). This is primarily due to the polymer flow within the nozzle being radially asymmetrical. Visual observations revealed the flow closest to where the polymer enters the heated block was slightly higher than flow near the centreline. The wall thickness varied due to imperfect alignment of the mandrel. This will be improved in future designs.

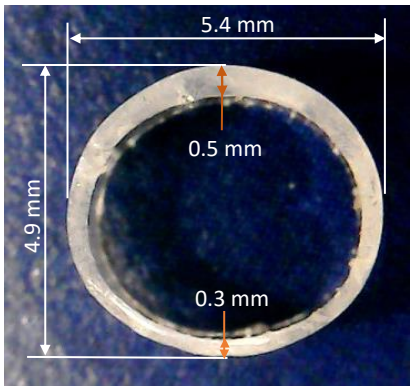

Figure 7. Printed tube cross-section T = 180°C, E = 130 mm/min, F = 0.8 mm/s.

Tests revealed that high feed rates, relative to the extrusion rate, reduces the tube diameter and eccentricity. Full results from the parameter tests are shown in Table 1. Mean radius for the ellipse is calculated using Eq. (3).

$$r_m = (2a + b)/3 \tag{3}$$

Table 1. Results of the print parameter tests on tube diameters.

Temperature, T, (°C)	Extrusion rate, E, (mm/min)	Feed rate, F, (mm/s)	Major axis, a, (mm)	Minor axis, b (mm)	Mean radius, r_m, (mm)
185	130	0.5	3.2	2.85	3.1
195	208	0.8	3.1	2.65	3.0
195	260	1.0	3.05	2.55	2.9
180	130	0.8	2.7	2.45	2.6
180	130	1.0	2.5	2.35	2.5
180	130	0.3	3.7	3.45	3.6
180	130	1.3	2.3	2.25	2.3

Eq. (4) is an empirical model, calculated using multiple linear regression, which can be used to predict the mean tube radius based on T, E and F.

$$r_m = 2.388 - 0.002465T + 0.003959(E/F) \quad (4)$$

Figure 8 demonstrates the accuracy of the equation which has an R^2 value of 0.9774.

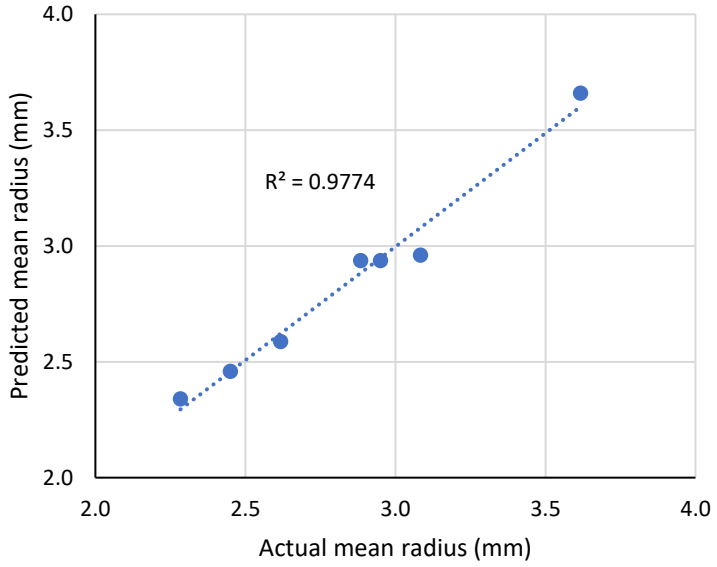

Figure 8. Actual vs predicted mean radius using Eq. (4).

Whilst the feed rate (nozzle speed) is much lower than seen in conventional FFF printing this is primarily because the cross section of the tube is much greater than that of a typical 0.4mm diameter nozzle. The volumetric extrusion rate in the parameter test ranges from 5.2mm^3/s to 10.4mm^3/s which is similar to that of extruders using conventional 0.4mm nozzles.

Positioning the extruder nozzle at an angle to the direction of travel increases the eccentricity of the tube. Once the nozzle is angled over 75° from the toolpath direction the tube tends to collapse (Figure 9 left). The collapsed tubes are still robust but lack consistent geometry. A 12V 0.1A 40mm radial fan running at 100% was found to provide enough internal pressure to prevent tube collapse (Figure 9 right). The maximum static pressure of the fan is 52Pa. However, care must be taken to prevent the tube wall getting too thin and perforating. A vacuum can be used to collapse the tube to form a ribbon.

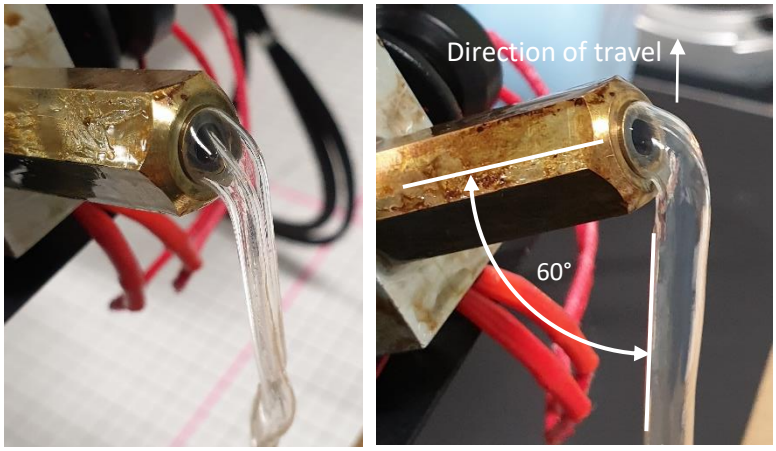

Figure 9. Nozzle orientated at 120° from travel direction. Left: Tube collapses without internal pressure. Right: No tube collapse when internal fan pressure is applied.

4. Mechanical testing

AMTEx parts may rely on the strength of the individual tubes or on the bonds between the tubes. The mechanical tests outlined in this section aim to assess both the strength of AMTEx tubes against tubes printed using conventional layer based FFF, and the strength of inter-tube bonds. All AMTEx tubes used in the tests were printed with PLA, Temperature = 185℃, Extrusion rate = 130mm/min, Feed rate = 0.5mm/s.

The AMTEx tubes were compared with FFF tubes with near identical geometries. The FFF tubes were printed both vertically and horizontally with 0.2mm layer heights and 0.4mm nozzles. All specimens were printed in triplicate.

4.1 Tensile tests

The tensile tests were performed on a Testometric 100 KN universal testing machine. Custom 3D printed adapters and inserts were used to grip the tubes without crushing the ends of the samples.

Figure 10. Tube tensile test apparatus with compliant fixtures to prevent tube collapse.

The results of the tensile tests are shown in Figure 11. The stiffness of the AMTEx tubes were indistinguishable from the conventionally printed (FFF) tubes but exhibited higher strength and

ductility. This conforms with established knowledge, as printed layers are known to introduce weaknesses into FFF parts.

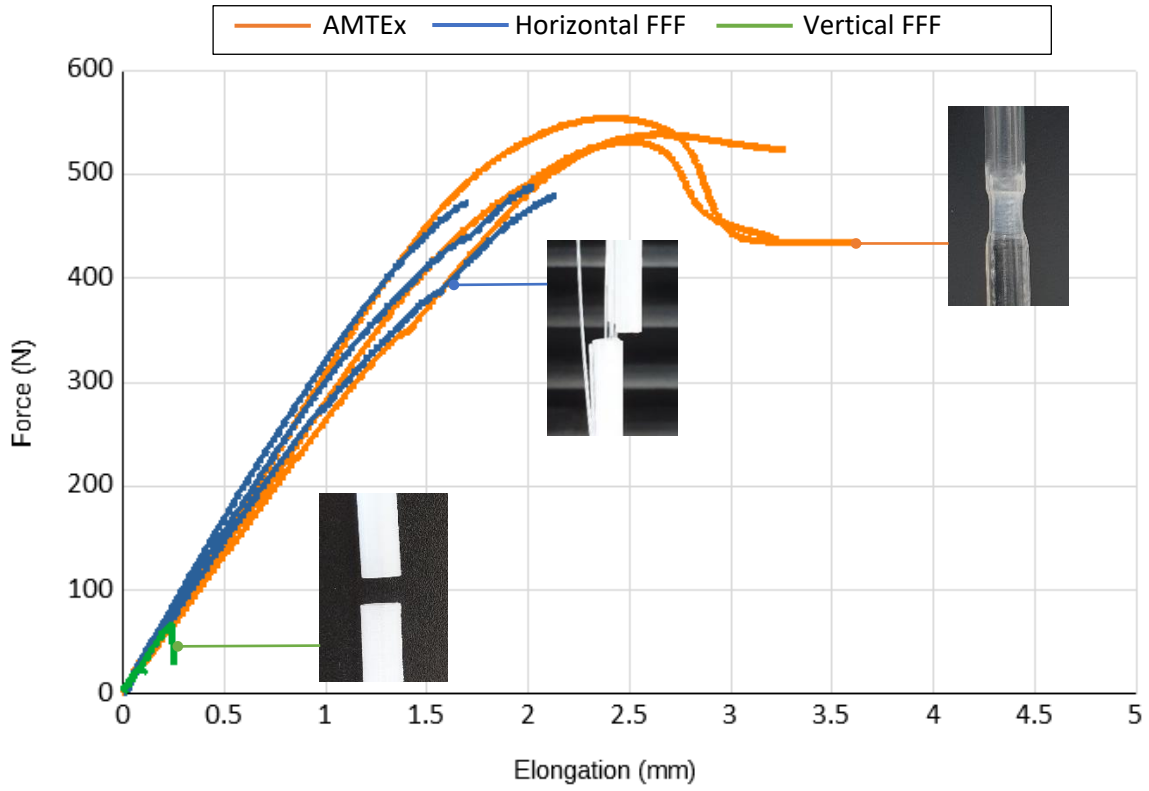

Figure 11. Tensile test results with inserts showing failed specimens.

The calculated average tensile strength of the AMTEx tubes is 62 MPa which is within the commonly quoted range of 55-65 MPa for PLA. The tensile strength of the conventional FFF tubes is 55 MPa and 6 MPa for the horizontally and vertically printed specimens respectively.

4.2 Bending tests

The 3-point bending tests were carried out using an Instron 34TM-50 with an 80 mm support span (Figure 12).

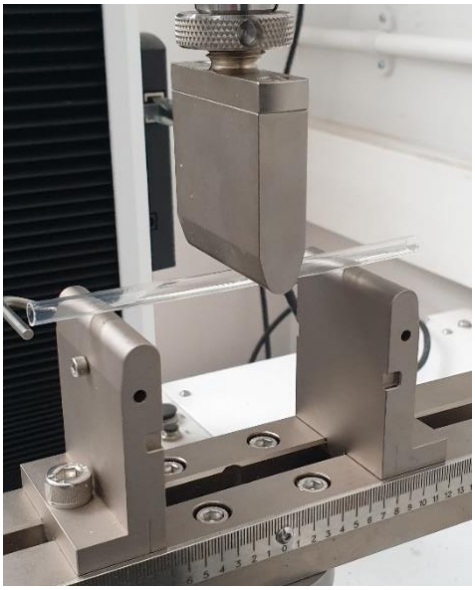

Figure 12. 3-point bending test apparatus.

The bending tests showed the AMTEx tubes to have equivalent stiffness to the FFF tubes, but increased strength and ductility (Figure 13).

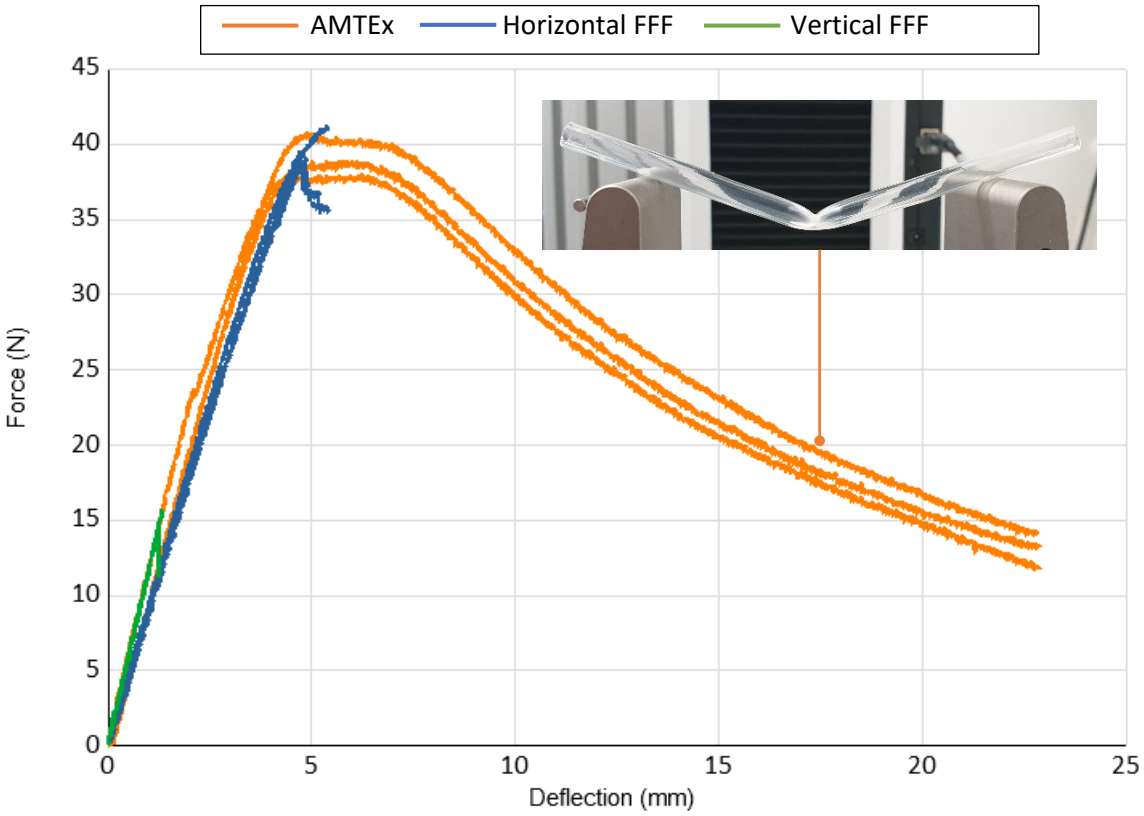

Figure 13. Results of the tube bending tests.

The calculated average flexural strength for both the AMTEx and horizontal FFF tubes is 69 MPa. This is similar to other values found for 3D printed PLA from literature [18]. The AMTEx tube failed due to buckling of the thin wall which is a likely reason for the flexural strength being below the commonly quoted value of 108 MPa for bulk PLA.

4.3 AMTEx tube bonding tests

To build up larger structures from tubes, it will be necessary for them to have strong interfacial bonds. Two tests were designed to test bond strength, a peel test (to test bonding between parallel tubes) and a twist test (to test bonding between orthogonal tubes). The toolpaths were designed to prevent the nozzle from contacting the previously deposited tube. Printing of the specimens can be seen in Figure 14a & 14c. The results of both tests indicate the bond between the tubes is not the weakest point in the specimens, and failure within tubes is likely to occur before failure of the inter-tube bonds.

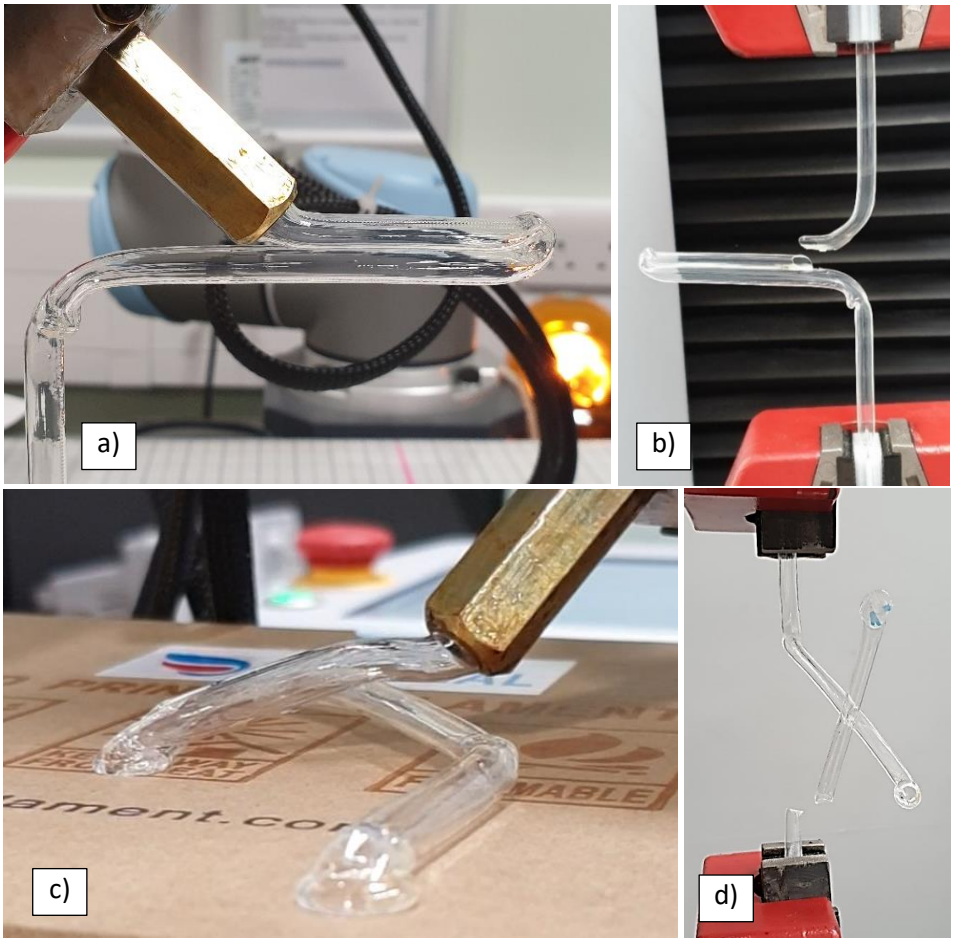

Figure 14. a) & c) Printing of the bonding test specimens. b) & d) Failure modes of the tests.

5. AMTEx artifacts

This section presents a small selection of objects printed using the AMTEx method. Online programming of the robot was achieved using the teach pendant while offline programming was achieved using Slic3r and RoboDK.

Figure 15 demonstrates printing with the nozzle at 90° to the toolpath and internal pressurisation of the tube. The letters 'UCLAN' were written in air, spanning approximately 400mm from the attachment point. Even though the toolpath includes 180° switchbacks and sharp corners the tube did not close and is watertight. Subsequent testing showed it was possible to close the tubes by applying suction to the inside of the tube. This suggests airtight chambers could be made by alternating between positive and negative pressure in the tube. It may also be possible to

dynamically vary the tube diameter by varying the pressure, although this was not explored in this study.

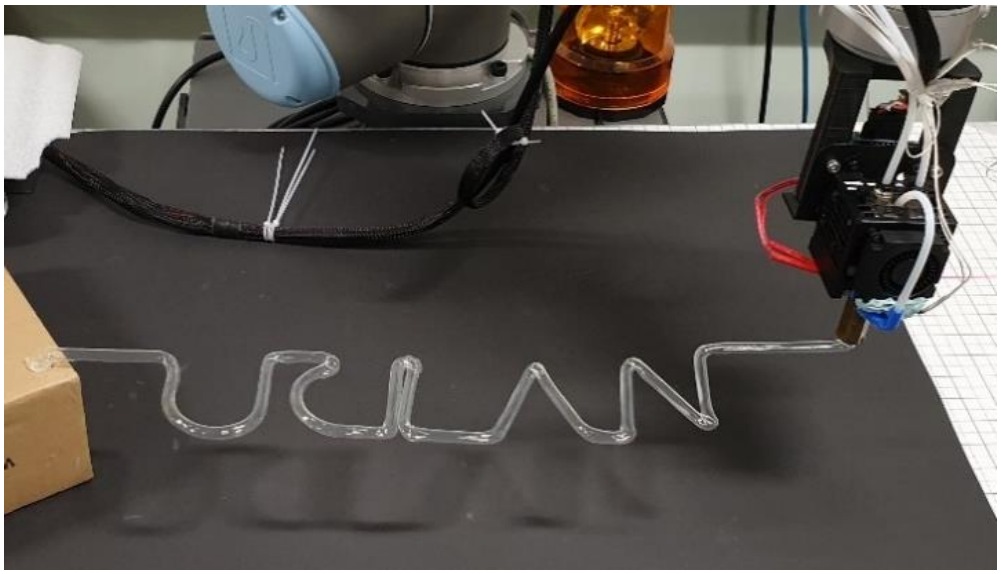

Figure 15. Demonstrating the freeform capabilities of AMTEx by printing the letters UCLAN in air, only supported from one small attachment point at the beginning of the print. Due to the nozzle being at 90° to the toolpath, internal tube pressurisation was required.

Figure 16 demonstrates the printing of a complex curve in air without internal tube pressurisation. The printed tube was remarkably stable; sagging due to gravity was visually imperceptable over the duration of the print. The tube was very lightweight and resisted firm pressure when held in a pinch grip.

Figure 16. Freeform printing of a self-supporting spiral tube. No internal tube pressurisation required.

Printing with the nozzle at 90° to the toolpath is especially useful, as it allows conventional print strategies and build preparation software to be used. To test this method, a vase was printed using Slic3r and RoboDK (Figure 17).

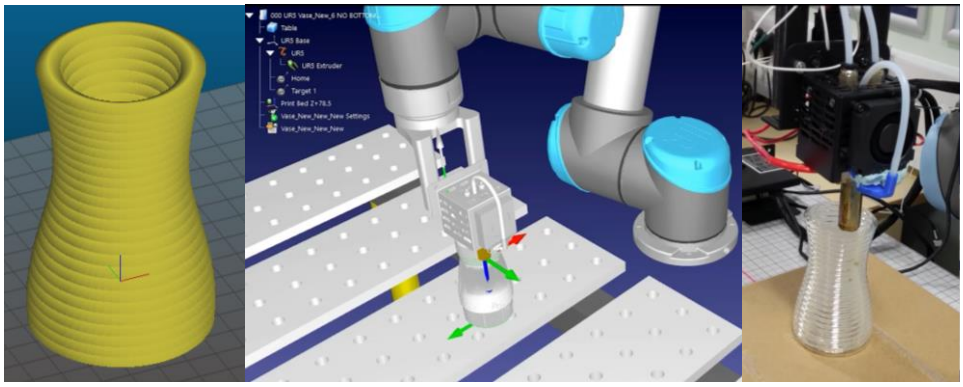

Figure 17. Demonstration of using Slic3r and RoboDK for off-line programming of the robot.

The printed vase geometry matches the CAD model well, however the horizontal dimensions are slightly reduced (Figure 18). This is likely due to the circular motion of the nozzle slightly dragging the tube into the centre.

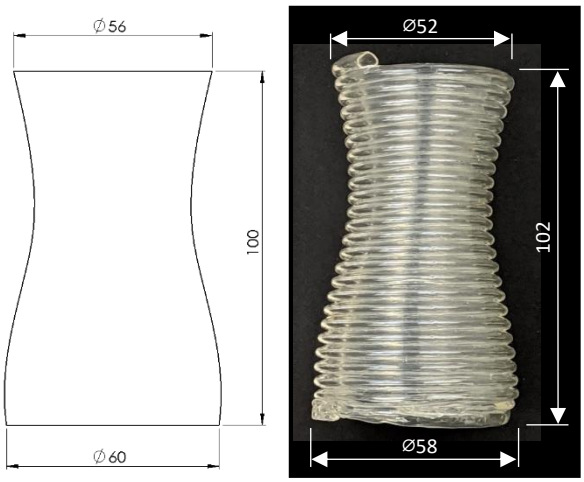

Figure 18. Comparison of CAD model dimensions with the AMTEx vase.

The vase was printed with a tube (approximately 8mm wide) using spiral vase mode with 4mm layer height. Figure 19 shows how the tubes conform to the geometry of the lower layer. This increases the contact area between layers. Despite the irregular shape of the cross-section the tube walls have consistent wall thicknesses.

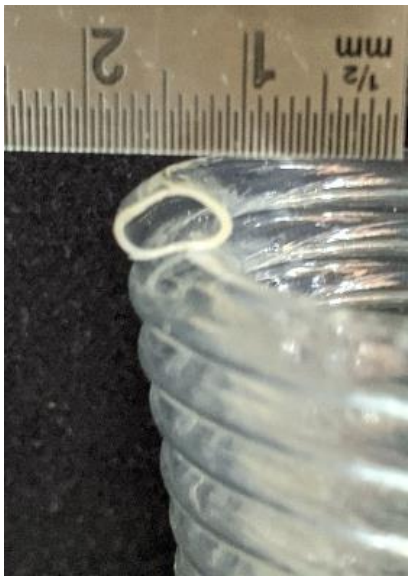

Figure 19. Close-up cross-section of a tube.

6. Discussion

The design of the tube extruder was sufficient to test and demonstrate the AMTEx technique however potential improvements were identified. Increasing the height of the heater block will increase the length of the melt zone, allowing higher volumetric extrusion rates. No active part cooling was used to solidify the tubes in this study. However, this will be required when printing with higher feed rates to prevent sagging, especially when printing tubes with thicker walls.

The parameter study demonstrated the possibility of controlling tube size by varying the extrusion rate, feed rate and print temperature. Balancing the feed rate with the extrusion rate was found to

be the most important factor for printing stable self-supporting tubes. Slight tension within the extrudate helped to produce smooth consistent tubes.

The mechanical properties of AMTEx tubes were found to be superior to conventionally printed tubes due to the removal of layers. This allowed the tubes to have mechanical properties much closer to the bulk material properties of the polymer. Bonds between tubes are strong due to the way the new tubes conform to the tubes below, increasing contact surface area.

The vase demonstrates the potential for printing large parts with minimal material use. The specific material savings depends on the geometry of the nozzle and the print parameters. For the vase in section 5 the reduction in material use was 60% (as measured using areal analysis of Figure 19 in ImageJ software). The self-supporting nature of AMTEx structures are best appreciated by watching the printing process. Time-lapse videos of each of the printed artefacts can be found in the supplementary materials (accessible electronically here).

With the option of layer-based printing or free-form printing, AMTEx allows for interesting hybrid print strategies. For example, layer-based printing could be used for the body or shell of an object, while free-form printing could be used to add features such as handles or strengthening ribs.

AMTEx parts may be used for thermal insulation or buoyancy. Alternatively, the tubes could be used to transport fluids or be filled with a range of materials such as resins, reinforcement fibres or flame retardants [19, 20]. The tubes also have interesting optical properties and may function as light guides or lighting fixtures [12, 21].

7. Conclusions and future work

The increased surface area of extruded tubes allows for superior cooling, reduced material use and freeform printing. Continuously extruded tubes have high specific bending and torsion strength and improved ductility over FFF tubes. Parallel and perpendicular inter-tube bonds were found to be strong enough that the tubes fracture before the inter-tube bonds.

Positive air pressure inside the printed tubes helps to prevent tube collapse even when the nozzle axis was over 120° from the toolpath. This makes it possible to print AMTEx parts using commonly available three-axis 3D printers and toolpath generation software.

Future work will include: redesigning the extruder to increase tube size and provide higher volumetric flow; adding part cooling to allow faster solidification of the tubes and increased feed rates; testing of polymer materials (other than PLA), and finding applications for AMTEx that makes best use of hybrid build strategies and the unique geometrical, mechanical and aesthetic qualities of the parts.

Acknowledgements:

The authors of this paper would like to thank the University of Central Lancashire UK, for providing the resources for this study; as well as Phil Tranter, Geoff Hall, Xiao Yin Guan, Dennis Boyle, Steve Kirby and Stuart Crook for their valuable assistance.

This research did not receive any specific grant from funding agencies in the public, commercial, or not-for-profit sectors.

8. References

1. Al Jassmi, H., F. Al Najjar, and A.-H.I. Mourad, *Large-Scale 3D Printing: The Way Forward.* IOP Conference Series: Materials Science and Engineering, 2018. **324**: p. 012088.
2. Lim, S., et al., *Modelling curved-layered printing paths for fabricating large-scale construction components.* Additive Manufacturing, 2016. **12**: p. 216-230.
3. Post, B.K., et al., *Using Big Area Additive Manufacturing to directly manufacture a boat hull mould.* Virtual and Physical Prototyping, 2019. **14**(2): p. 123-129.
4. Khoshnevis, B., et al., *Mega-scale fabrication by Contour Crafting.* International Journal of Industrial and Systems Engineering, 2006. **1**(3): p. 301-320.
5. Moreno Nieto, D., V. Casal López, and S.I. Molina, *Large-format polymeric pellet-based additive manufacturing for the naval industry.* Additive Manufacturing, 2018. **23**: p. 79-85.
6. Boyd, P., et al., *Design and Manufacturing of The First Freeform 3D-Printed House.* Proceedings of IASS Annual Symposia, 2019. **2019**(6): p. 1-7.
7. Google Trends. Search term: 'Large 3D printer' 24/03/2020]; Available from: https://trends.google.com/trends.
8. Roschli, A., et al., *Designing for Big Area Additive Manufacturing.* Additive Manufacturing, 2019. **25**: p. 275-285.
9. Byard, D.J., et al., *Green fab lab applications of large-area waste polymer-based additive manufacturing.* Additive Manufacturing, 2019. **27**: p. 515-525.
10. Go, J., et al., *Rate limits of additive manufacturing by fused filament fabrication and guidelines for high-throughput system design.* Additive Manufacturing, 2017. **16**: p. 1-11.
11. Cornock, R., S. Beirne, and G.G. Wallace. *Development of a Coaxial Melt Extrusion Printing process for specialised composite bioscaffold fabrication*. in *2013 IEEE/ASME International Conference on Advanced Intelligent Mechatronics*. 2013.
12. Talataisong, W., et al., *Novel method for manufacturing optical fiber: extrusion and drawing of microstructured polymer optical fibers from a 3D printer.* Optics Express, 2018. **26**(24): p. 32007-32013.
13. Laarman, J., et al., *Anti-gravity additive manufacturing.* Fabricate 2014: Negotiating design & making, 2014: p. 191-197.
14. Shelton, T., *Cellular Fabrication.* Technology|Architecture + Design, 2017. **1**(2): p. 251-253.
15. Cardno, C.A., *Robotic Printing Conquers a New Material: Stainless Steel.* Civil Engineering Magazine Archive, 2018. **88**(9): p. 36-37.
16. Ray, A.K., et al., *Bamboo—A functionally graded composite-correlation between microstructure and mechanical strength.* Journal of Materials Science, 2005. **40**(19): p. 5249-5253.
17. Urhal, P., et al., *Robot assisted additive manufacturing: A review.* Robotics and Computer-Integrated Manufacturing, 2019. **59**: p. 335-345.
18. Kuznetsov, V.E., et al., *Strength of PLA Components Fabricated with Fused Deposition Technology Using a Desktop 3D Printer as a Function of Geometrical Parameters of the Process.* Polymers, 2018. **10**(3): p. 313.
19. Brooks, H. and S. Molony, *Design and evaluation of additively manufactured parts with three dimensional continuous fibre reinforcement.* Materials & Design, 2016. **90**: p. 276-283.
20. Brooks, H., et al., *Fire resistance of additively manufactured water filled polymer parts.* Additive Manufacturing, 2018. **22**: p. 138-145.
21. Canning, J., et al., *Drawing optical fibers from three-dimensional printers.* Optics Letters, 2016. **41**(23): p. 5551-5554.